

How metal ions link in Metal-Organic Frameworks: dots, rods, sheets, and 3D Secondary Building Units exemplified by a Y(III) 4,4'-oxydibenzoate

Cyrielle L.F. Dazem,^{a,b} Niklas Ruser,^a Erik Svensson Grape,^c A. Ken Inge,^c Davide M. Proserpio,^d Norbert Stock*^a and Lars Öhrström*^e

^a Institute of Inorganic Chemistry, Christian-Albrechts University of Kiel, Max-Eyth-Straße 2, 24118 Kiel, Germany

^b Inorganic Chemistry Department, University of Yaoundé 1, P.O. Box 812, Yaoundé, Cameroon

^c Department of Materials and Environmental Chemistry, Stockholm University, 10691, Stockholm, Sweden

^d Dipartimento di Chimica, Università degli studi di Milano, Via Golgi 19, 20133 Milano, Italy

^e Chemistry and Biochemistry, Dept. of Chemistry and Chemical Engineering, Chalmers University of Technology, SE-41296 Gothenburg, Sweden.

Table of contents

YOBA composition and activation.....	2
Materials and Methods.....	2
Synthetic Procedures.....	2
SCXRD.....	3
Table S1. SCXRD Experimental details.....	3
PXRD.....	4
Fig. S1: Comparison of the powder patterns of 1 (black) and 2 (red).....	4
Fig. S2: Pawley-Fit of 1	4
Fig. S3: Pawley-Fit of 2	5
Tab. S2: Results of the Pawley-Fits of the compounds 1 and 2	5
TG.....	6
Fig. S4: TG and DTA data of $[Y_{16}(\mu-OH_2)(\mu_3-OH)_8(oba)_{20}(dmf)_4] \cdot 6 H_2O \cdot 6 dmf$ (1 ·6 H ₂ O·6 dmf) 1	6
Tab. S3: Measured and calculated mass loss steps of the TG data of $[Y_{16}(\mu-OH_2)(\mu_3-OH)_8(OBA)_{20}(DMF)_4] \cdot 5 H_2O \cdot 6 DMF$	6
Fig. S5: TG and DTA data of $[Y_{16}(\mu-OH_2)(\mu_3-OH)_8(oba)_{20}] \cdot 3H_2O$ (2 ·3H ₂ O).	7
Tab. S4: Comparison of measured and calculated mass steps of the TG measurement of $[Y_{16}(\mu-OH_2)(\mu_3-OH)_8(oba)_{20}] \cdot 3H_2O$	7
Fig. S6: TG of 1 (black) and 2 (red).....	7
Fig. S7: PXRD data of the residues of 1 (red) and 2 (blue) after the TG measurements compared to the calculated powder pattern of Y ₂ O ₃ (black). ^[1]	8
IR.....	9
Fig. S8: Comparison of the IR spectra of 1 (black) and 2 (red).....	9
Gas sorption analysis.....	10
Figure S9 CO ₂ adsorption isotherm of 2 at 298 K.....	10
Mercury pore analysis of 1 and calculations of CO ₂ loading with the 50% rule.....	10
Literature.....	11

YOBA composition and activation

The composition of the compound based on the crystal structure determination is $[Y_{16}(\mu\text{-OH}_2)(\mu_3\text{-OH})_8(\text{oba})_{20}(\text{dmf})_4] = \mathbf{1}$. Elemental analysis and TG analysis show that different amounts of guest molecules are present in the pores. While elemental analysis leads to a composition of $[Y_{16}(\mu\text{-OH}_2)(\mu_3\text{-OH})_8(\text{oba})_{20}(\text{dmf})_4] \cdot 7\text{H}_2\text{O} \cdot 7\text{dmf}$, evaluation of the TG curve results in $[Y_{16}(\mu\text{-OH}_2)(\mu_3\text{-OH})_8(\text{oba})_{20}(\text{dmf})_4] \cdot 5\text{H}_2\text{O} \cdot 6\text{dmf}$. This is probably also due to the different relative humidity values and the flow of air in the TG analysis.

$[Y_{16}(\mu\text{-OH}_2)(\mu_3\text{-OH})_8(\text{OBA})_{20}] = \mathbf{2}$ is obtained by thermal treatment of **1**. The adsorbed and coordinated dmf molecules were removed while the structure is preserved which was confirmed by a Pawley fit. From elemental analysis the absence of N atoms in the sample is confirmed, the compound adsorbs water, and the elemental analysis leads to the composition $[Y_{16}(\mu\text{-OH}_2)(\mu_3\text{-OH})_8(\text{OBA})_{20}] \cdot 6\text{H}_2\text{O}$. TG analysis results in the composition $[Y_{16}(\mu\text{-OH}_2)(\mu_3\text{-OH})_8(\text{OBA})_{20}] \cdot 3\text{H}_2\text{O}$. This is probably also due to the different relative humidity values and the flow of air in the TG analysis.

Materials and Methods

All used materials and solvents were used without further purification. $Y(\text{NO}_3)_3 \cdot 6\text{H}_2\text{O}$ (99.9 % Y) was purchased from abcr, 4,4'-oxydibenzoic acid (>98 %) was obtained from TCI and *N,N*-dimethylformamide (99 %) was obtained from Grüssing. For the characterization of the products PXRD patterns were collected on a STOE Stadi P diffractometer equipped with a MYTHEN2 1K detector and using $\text{Cu K}\alpha_1$ radiation. The measurements were performed with a flat sample holder in transmission geometry. TG and DTA measurements were conducted on a Linseis STA PT 1000 (heating rate = 4 K/min, airflow = 6 L/h). Sorption measurements were performed using a MICROTRAC BELSORP MINI X with CO_2 at 298.15 K. For activation prior to the sorption measurement the sample was treated for 20 h at a temperature of 200 °C under reduced pressure (<10 Pa). The title compound was synthesized using a custom-made steel autoclave (total volume 2 mL for each insert) using a programmable Memmert UFP 400 oven with forced ventilation using a defined temperature-time program. CHNS data was collected using a vario MICRO cube Elementaranalysator from Elementar.

Synthetic Procedures

For the synthesis of **1** 16.2 mg (0.063 mmol) 4,4'-oxydibenzoic acid (H_2oba , TCI, 98 %) and 24.0 mg (0.063 mmol) $Y(\text{NO}_3)_3 \cdot 6\text{H}_2\text{O}$ (abcr, 99.9 %) were transferred into a 2 mL Teflon vessel. 200 μL H_2O and 800 μL DMF were added. The Teflon vessel was placed into and sealed in a steel reactor. The reactor was heated to 170 °C within 2 h and the temperature was held for 16 h. The reactor was cooled down to room temperature within 6 h. The precipitated product was filtered off, washed with 3 mL H_2O and dried in air. By heating **1** to 200 °C overnight at ambient pressure the coordinated DMF as well as the guest molecules located inside the pores could be removed leading to compound **2**.

Elemental analysis (**1**, $[Y_{16}(\mu\text{-OH}_2)(\mu_3\text{-OH})_8(\text{oba})_{20}(\text{dmf})_4] \cdot 7\text{H}_2\text{O} \cdot 7\text{dmf}$): measured/calculated: C = 49.26/49.26 %, H = 3.67/3.45 %, N = 2.07/2.02 %.

Yield: 13.2 mg (1.89 μmol , 48 %).

Elemental analysis (**2**, $[Y_{16}(\mu\text{-OH}_2)(\mu_3\text{-OH})_8(\text{oba})_{20}] \cdot 6\text{H}_2\text{O}$): measured/calculated: C = 49.34/49.39 %, H = 3.18/2.69 %, N = 0.00/0.00 %.

SCXRD

Table S1. SCXRD Experimental details

	YOBA
Crystal data	
Chemical formula	C ₂₉₂ H ₁₈₈ N ₄ O ₁₁₃ Y ₁₆
M_r	6983.04
Crystal system, space group	Tetragonal, $I4_1$
Temperature (K)	297
a, c (Å)	28.1762 (6), 39.8472 (8)
V (Å ³)	31634.6 (15)
Z	4
Density	1.4662 g/cm ³
Radiation type	Cu $K\alpha$
μ (mm ⁻¹)	4.48
Crystal size (mm)	0.04 × 0.04 × 0.03
Data collection	
Diffractometer	Bruker D8 Venture
Absorption correction	Multi-scan, Sheldrick, G. M. (1996). <i>SADABS</i> . University of Göttingen, Germany.
T_{\min}, T_{\max}	0.642, 0.753
No. of measured, independent and $\left[\begin{smallmatrix} I \\ SFP \end{smallmatrix} \right]$ observed [$I > 2s(I)$] reflections	48770, 21077, 15557
R_{int}	0.105
$(\sin \theta)_{\text{max}}$ (Å ⁻¹)	0.588
Refinement	
$R[F^2 > 2s(F^2)], wR(F^2), S$	0.055, 0.121, 0.99
No. of reflections	21077
No. of parameters	1919
No. of restraints	463
H-atom treatment	H-atom parameters constrained
$D\rho_{\text{max}}, D\rho_{\text{min}}$ (e Å ⁻³)	1.19, -0.85
Absolute structure	Refined as an inversion twin.
Absolute structure parameter	0.008 (19)

Computer programs: *SHELXT* 2014/5 (Sheldrick, 2014), *SHELXL2018/1* (Sheldrick, 2018).

PXRD

Upon thermal activation, compound **1** undergoes a phase transformation to a DMF free form **2** (Fig. S1). The powder pattern of **1** (Fig. S2) was successfully fitted by a Pawley fit starting from single crystal data. It was possible to conduct a Pawley fit on the powder data of **2** (Fig. S3) with the initial cell parameters and space group of **1** which resulted in a smaller cell volume (Tab. S).

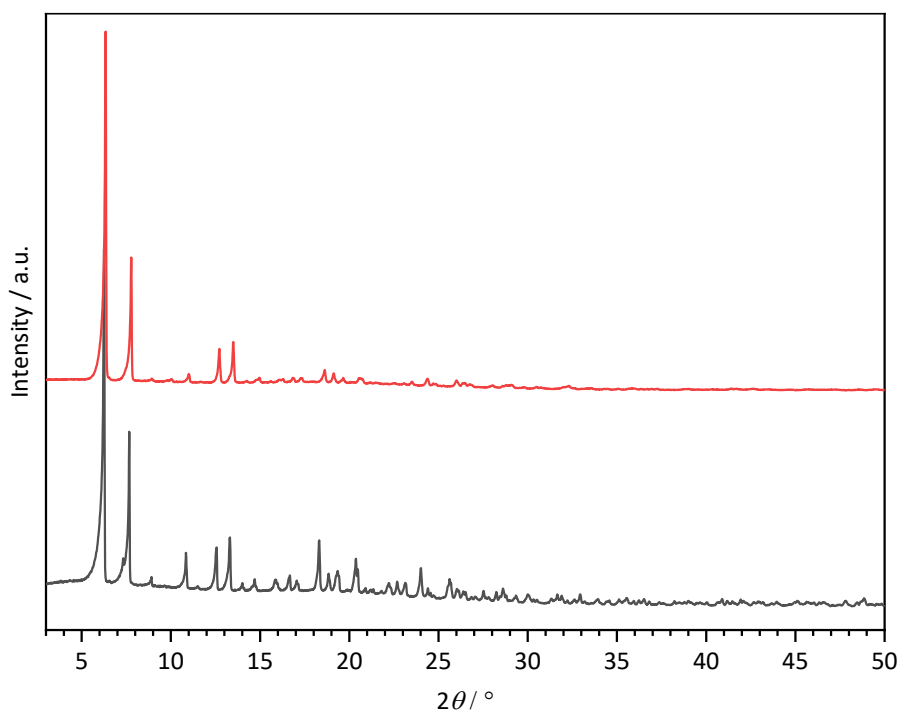


Fig. S1: Comparison of the powder patterns of **1** (black) and **2** (red).

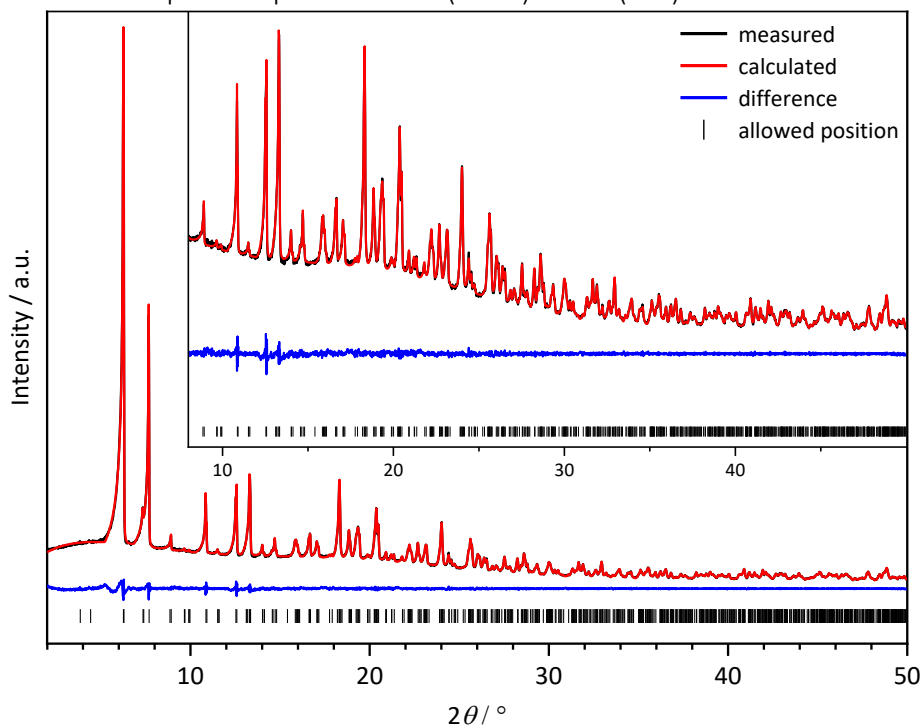


Fig. S2: Pawley-Fit of **1**.

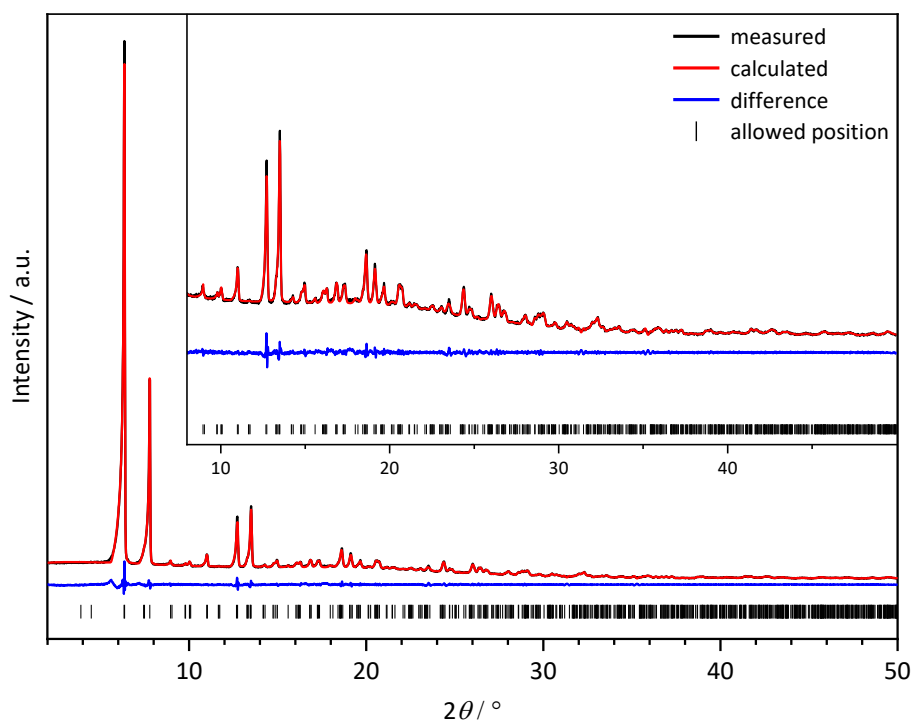


Fig. S3: Pawley-Fit of 2.

Tab. S2: Results of the Pawley-Fits of the compounds 1 and 2.

Parameter	$[Y_{16}(\mu\text{-OH}_2)(\mu_3\text{-OH})_8(\text{OBA})_{20}(\text{DMF})_4]$ (1)	$[Y_{16}(\mu\text{-OH}_2)(\mu_3\text{-OH})_8(\text{OBA})_{20}]$ (2)
Space group	$I4_1$	$I4_1$
$a=b$ / Å	28.2249(14)	27.911(9)
c / Å	39.602(17)	39.140(9)
Volume / Å ³	31548(4)	30490(19)
R_{wp} / %	2.19	2.96
GoF / %	0.69	0.66

TG

The TG measurement of **1** shows that between room temperature and 89 °C water is released. This is followed by a loss of DMF in the range of 89–261 °C. Above 320 °C the OBA linker starts to decompose leaving Y_2O_3 as residue behind (Fig. S7).

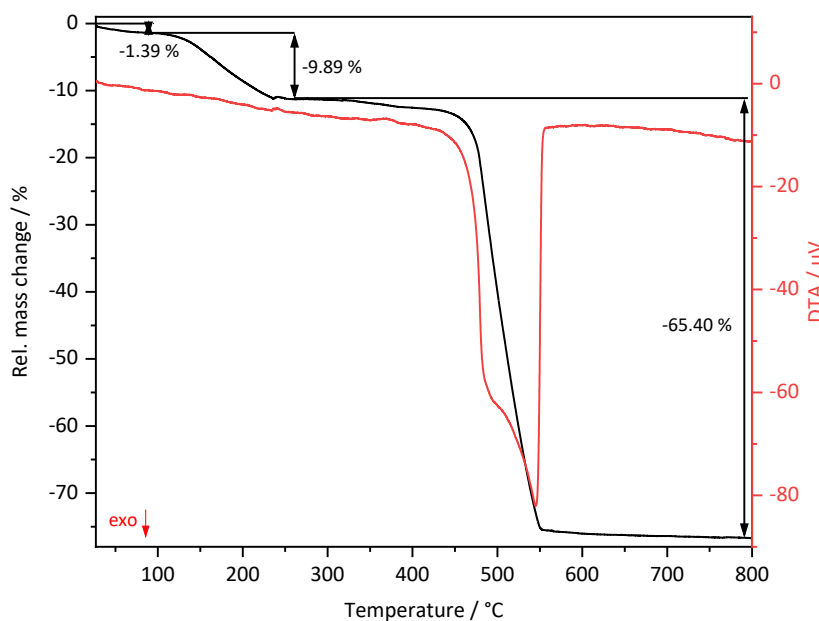


Fig. S4: TG and DTA data of $[Y_{16}(\mu\text{-OH}_2)(\mu_3\text{-OH})_8(\text{oba})_{20}(\text{dmf})_4] \cdot 6 \text{H}_2\text{O} \cdot 6 \text{dmf}$ (**1**·6 H_2O ·6 dmf) **1**.

Tab. S3: Measured and calculated mass loss steps of the TG data of $[Y_{16}(\mu\text{-OH}_2)(\mu_3\text{-OH})_8(\text{OBA})_{20}(\text{DMF})_4] \cdot 5 \text{H}_2\text{O} \cdot 6 \text{DMF}$.

Mass step	measured / %	calculated / %	
Step 1	-1.39	-1.43	6 H_2O
Step 2	-9.89	-9.69	10 DMF
Step 3	-65.40	-64.91	20 OBA
Residue	23.32	23.96	8 Y_2O_3

The TG data of **2** reveals a mass loss of 1 % between room temperature and 127 °C, which we assign to re-adsorbed water molecules. No mass loss step at higher temperatures which would be typical for the loss of DMF was observed for **2** so the thermal treatment of **1** indeed leads to the DMF free form. At approximately 420 °C the compound starts to decompose which results in Y_2O_3 as the residue.

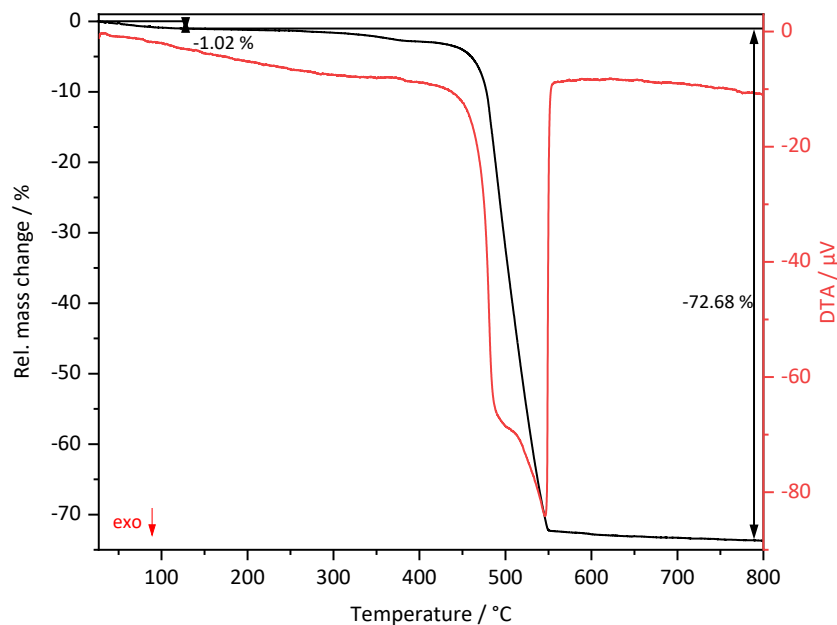


Fig. S5: TG and DTA data of $[Y_{16}(\mu\text{-OH}_2)(\mu_3\text{-OH})_8(\text{oba})_{20}] \cdot 3\text{H}_2\text{O}$ ($2 \cdot 3\text{H}_2\text{O}$).

Tab. S4: Comparison of measured and calculated mass steps of the TG measurement of $[Y_{16}(\mu\text{-OH}_2)(\mu_3\text{-OH})_8(\text{oba})_{20}] \cdot 3\text{H}_2\text{O}$.

Mass step	measured / %	calculated / %	
Step 1	-1.02	-1.06	4 H ₂ O
Step 2	-72.68	-72.26	20 OBA
Residue	26.30	26.67	8 Y ₂ O ₃

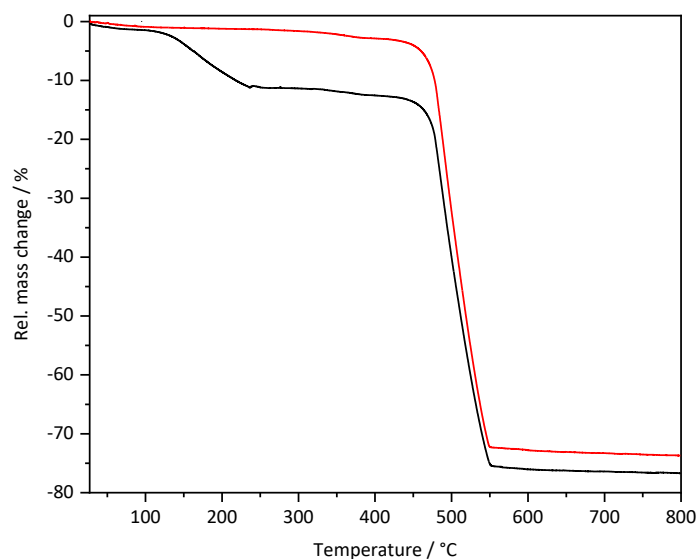


Fig. S6: TG of **1** (black) and **2** (red).

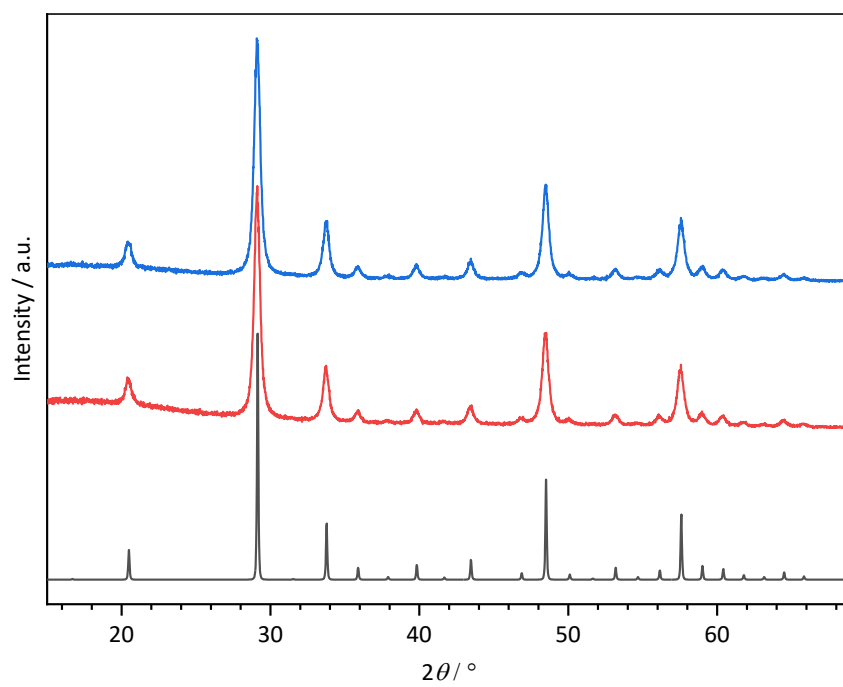


Fig. S7: PXRD data of the residues of **1** (red) and **2** (blue) after the TG measurements compared to the calculated powder pattern of Y_2O_3 (black).^[1]

IR

IR spectra of compounds **1** and **2** differ only due to additional bands caused by the presence of dmf molecules in **1** which are absent in **2**. The band at 2927 cm^{-1} is caused by the stretching vibrations of the $-\text{CH}_3$ groups^[2] and the band at 1663 cm^{-1} can be assigned to the $\text{C}=\text{O}$ moiety (stretching vibration)^[3] of dmf molecules. Another band at 1625 cm^{-1} is located at too low wave numbers for $\text{C}=\text{O}$ groups but is possibly caused by dmf molecules interacting with the framework. The O-H stretching vibration^[2] band at 3622 cm^{-1} can be observed in **1** and **2** and shows the existence of OH moieties which could be assigned to coordinated OH^- and H_2O molecules.

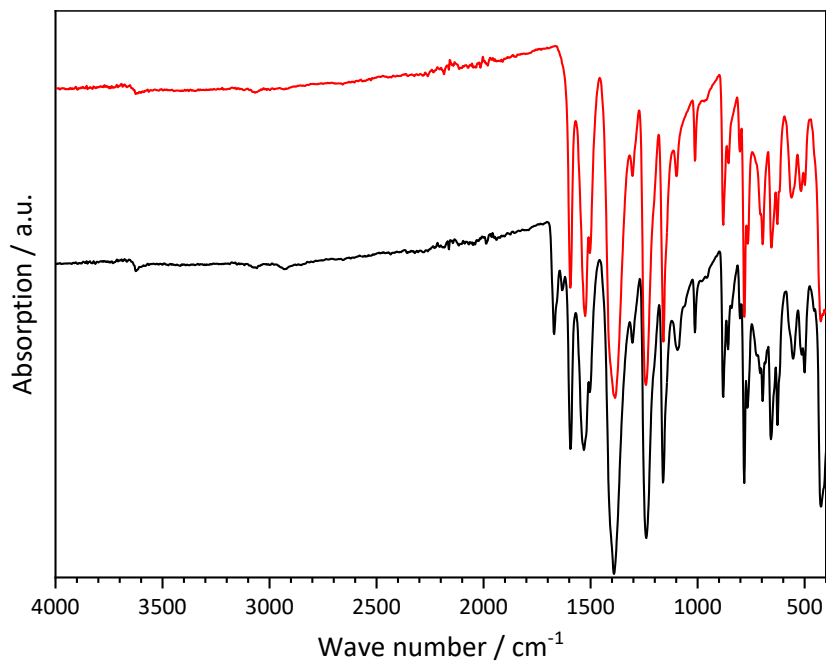


Fig. S8: Comparison of the IR spectra of **1** (black) and **2** (red).

Gas sorption analysis

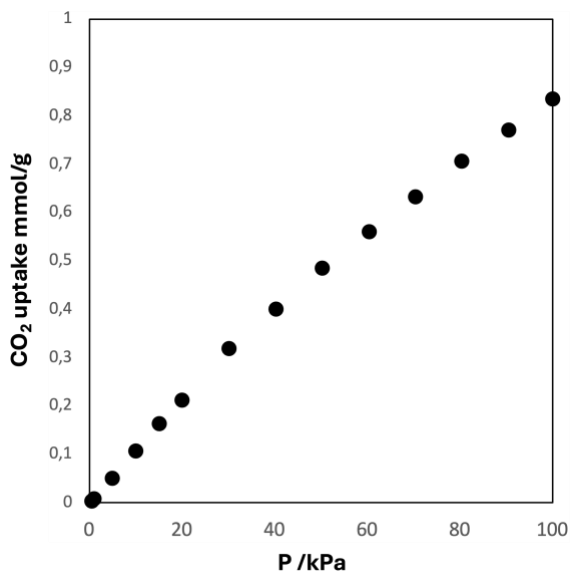


Figure S9 CO₂ adsorption isotherm of **2** at 298 K.

Mercury pore analysis of **1** and calculations of CO₂ loading with the 50% rule

Show

Probe Radius: Å

Approx. Grid Spacing: Å

Calculate using the Solvent Accessible Surface

Display Options

Outside Colour: 1

Inside Colour: 1

Results

Volume % of unit cell volume

Å³

Molecular volume of CO₂ is 38.30 Å³, number of CO₂ per unit cell can then be calculated according to the van Heerden & Barbour 50% rule of thumb[4] as: $0.5 \cdot 1311.32 / 38.30 = 17.12$. The density of **1** is 1.4662 g/cm³ and one unit cell has the volume 31634.622 Å³ = $3.16 \cdot 10^{-20}$ cm³. This gives CO₂ estimate per volume as $80 / 3.16 \cdot 10^{-20} = 5.411 \cdot 10^{20}$ CO₂ molecules per cm³, thus $5.411 \cdot 10^{20} / N_A$ moles/cm³ = $0.8986 \cdot 10^{-3}$ moles/cm³ which gives $0.8986 \cdot 10^{-3} / 1.4662$ moles/g = 0.61 mmol/g uptake of CO₂ comparable to the measured 0.85 mmol/g.

Literature

- [1] M. Faucher, J. Pannetier, *Acta Crystallogr., Sect. B* **1980**, *36*, 3209–3211.
- [2] G. Socrates, *Infrared and Raman Characteristic Group Frequencies*, John Wiley & Sons Ltd., Chichester, **2001**.
- [3] A. Shastri, A. K. Das, S. Krishnakumar, P. J. Singh, B. N. R. Sekhar, *J. Chem. Phys.* **2017**, *147*, 224305.